Seismic numerical modelling to monitor CO_2 storage in the Baltic Sea offshore structure

*Kazbulat Shogenov [a, b] and Davide Gei [b]

[a] Institute of Geology at Tallinn University of Technology, Ehitajate tee 5, Estonia

[b] Istituto Nazionale di Oceanografia e di Geofisica Sperimentale (OGS), Borgo Grotta Gigante, 42/c, 34010 Sgonico Trieste, Italy

Contacts
e-mail: shogenov@gi.ee
skype: kazbulat
GSM: +372 55 89 001

European Association of Geoscientists & Engineers
The 75th EAGE Conference & Exhibition
10-13.06.13, London, UK

Our research is a part of CO_2 capture and geological storage (CCS/CGS) study in the Baltic Region. We have applied **time-lapse 4D rock physics and seismic numerical modelling methodology to compute synthetic seismograms without and with CO_2** injected into a deep geological structure in the Baltic Sea Region and to design basis for further CGS monitoring plan in the region. This is an important technology to **predict the seismic response to the presence of CO_2 in the storage site**, to **monitor CO_2 plume migration and evolution within the reservoir, estimate reservoir integrity and support possible leakage notification**. We selected the most prospective offshore oil-bearing geological structure E6 suitable for trapping of CO_2 in the Latvian Baltic Sea Region **(Figs. 1, 2, 3)**. Deimena Sandstone Formation of Middle Cambrian was estimated as a high quality reservoir in the E6 anticline structure prospective for CO_2 storage (**Shogenov et al., 2013a, b**). Laboratory measurements of rock properties of reservoir sandstones measured at IFPEN laboratory **(Shogenov et al., 2013a)** were applied for modelling. For other layers above and below the storage formation velocities from active seismic

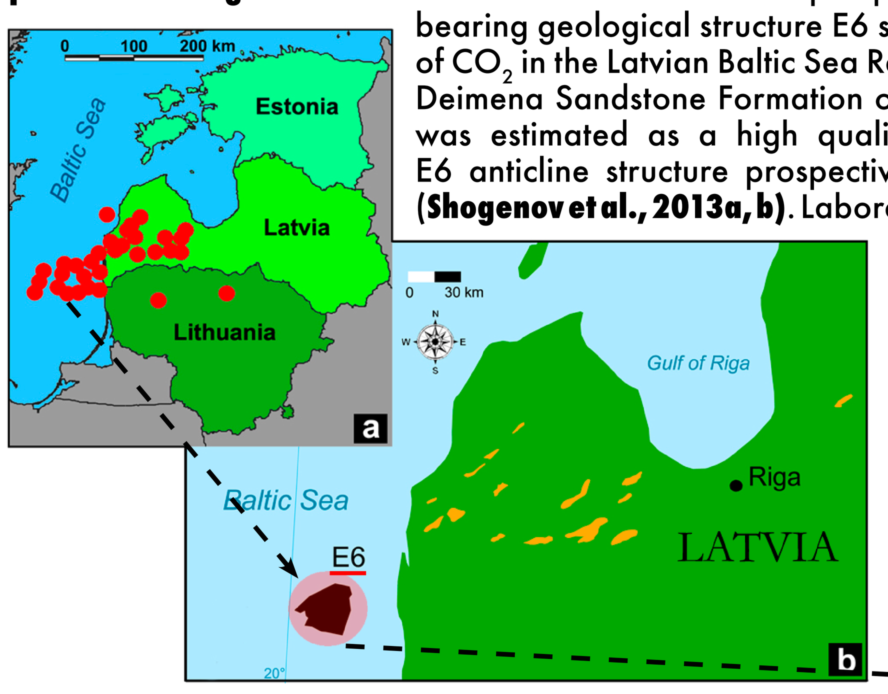

Fig. 1. (a) Approximate location of 16 onshore and 16 offshore Latvian structures in the Cambrian aquifer prospective for CGS (CO_2 storage potential exceeding 2 Mt), shown by red circles; **(b)** 16 onshore (orange) and studied E6 offshore structures (black) in Latvia. Red transparent circle shows location of the studied E6 offshore structure (maps built using ArcGis 9.2 software, **Shogenov et al., 2013b**)

I. INTRODUCTION

surveys published in the exploration report of the E6 structure and values of rock properties estimated from empirical relations were used. Geological model was constructed for the main formations **(Fig. 4)** and populated with petrophysical properties (temperature, pressure, solid rock composition, fluid saturation, porosity, density, seismic wave velocities and quality factors). The seismic properties of the reservoir with different saturation levels of CO_2 and their seismic responses were computed. Results were compared with initial conditions using difference sections and normalized root mean square (NRMS) methodology.

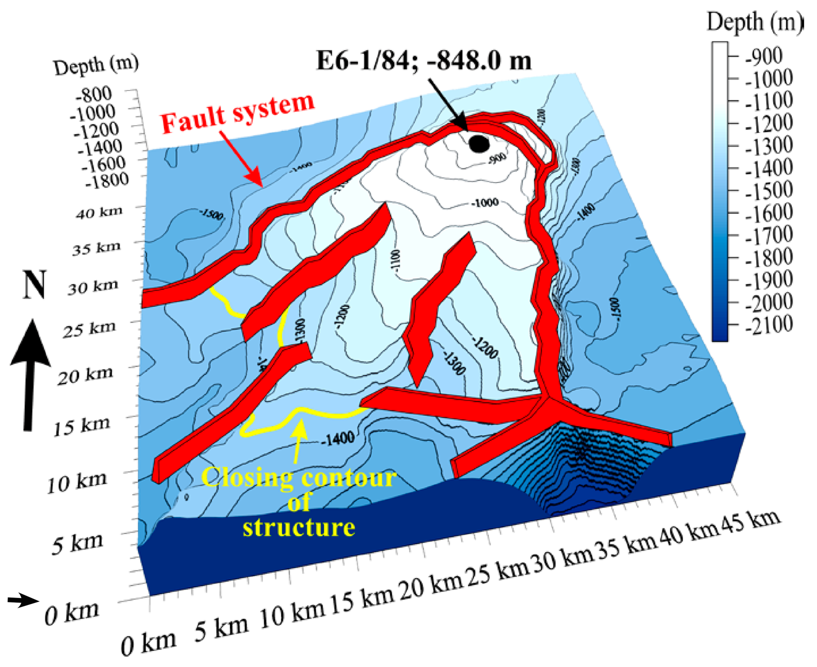

Fig. 2. 3D geological model of the top of the Deimena Formation in the E6 structure with the estimated closing contour of the structure (yellow contour -1350m). Faults bordering the structure are shown by a red walls. Location of the well is shown by a black circle with the depth of the top of the Deimena Formation (−848 m) (model was built in Surfer 8 software, **Shogenov et al., 2013a**)

Area: 600 km²
Thickness: 53 m
Salinity: 99000 ppm
Cap rock:
146 m Ordovician F. + 120 m Silurian F. (shales marlstones and limestones)

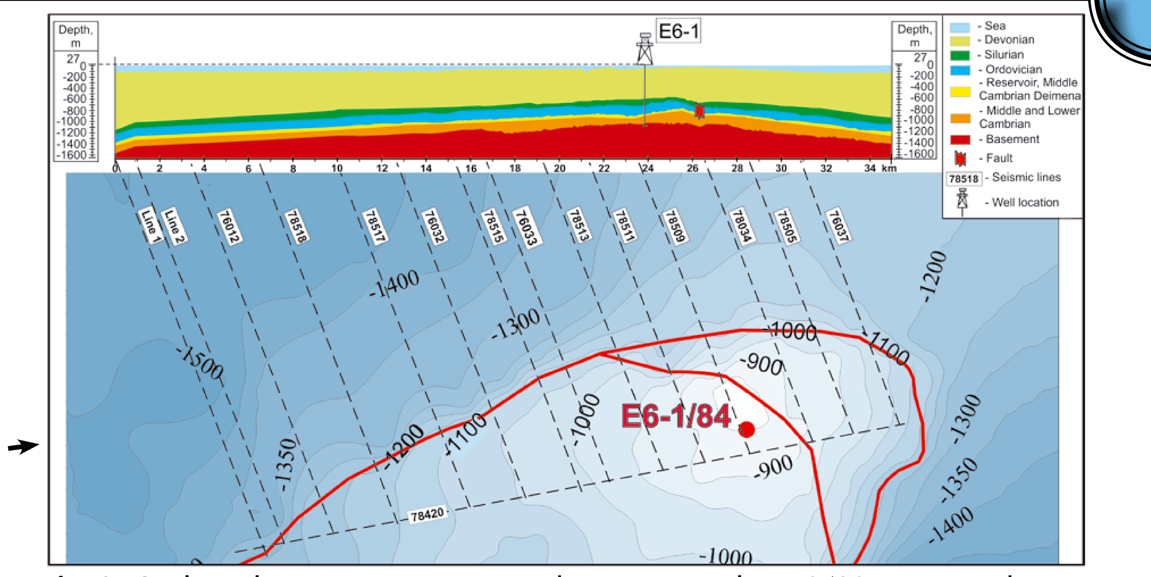

Fig. 3. Geological cross section corresponding to seismic line 78420, interpreted using reported seismic data, local structure map and lithological cross section in well E6-1/84 (**Shogenov et al., 2013b**).

Numerical mesh: 240000 (800 X 300) grid points
Grid spacing: 5 m
Absorbing boundaries: 40 grid-point lengths (bottom, left and right sides)

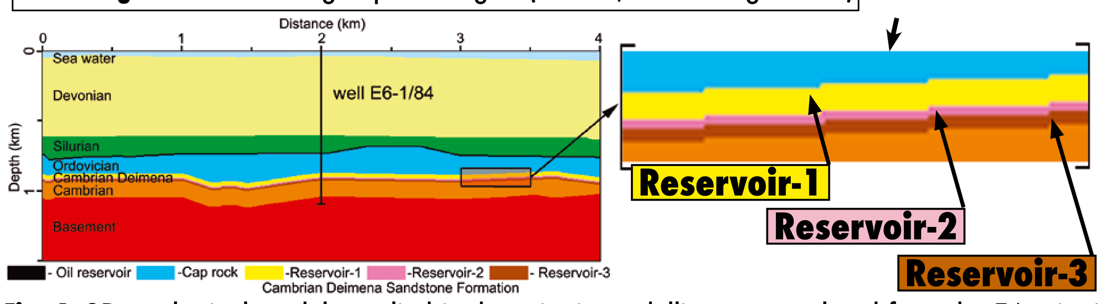

Fig. 4. 2D geological model, applied in the seismic modelling, extrapolated from the E6 seismic section **(Fig. 3)** with well E6-1/84 in the centre. Deimena Reservoir of Middle Cambrian was split into three parts according their specific physical properties (Reservoir -1, -2 and -3)

II. METHODOLOGY

2.1. PROPERTIES BEFORE CO_2 SATURATION

We set up a 2D model consisting of 10 main geological layers **(Fig.4)**. We implemented vertical heterogeneity within the reservoir layer and split the Middle Cambrian Deimena Reservoir into three parts (Reservoir-1, -2 and -3: yellow, pink and brown colours in the **Fig. 4**, respectively). In the horizontal direction the reservoir was estimated to be homogeneous. Thin 10 meters black coloured layer between Ordovician and Silurian formations is Upper Ordovician oil reservoir. All the formations are characterized by specific constant rock properties **(Table 1)**.

Table 1. Seismic and physical properties of main rock formations shown in the model **(Figure 4)**

Formation	Lithology	T (°C)	P (MPa)	ρ wet (kg/m³)	ϕ (%)	κ (mD)	V_P (m/s)	V_S (m/s)	Q_P	Q_S	μ (Gpa)	K (Gpa)
Sea water	-	10-7	0.1-0.8	1030	-	-	1480	0	-	-	-	-
Devonian	Sandstone	7-31	0.8-6.3	2226	15	2	2474	1133	66	18	2.9	-
Silurian (Extra Cap rock)	Claystone	31-35	6.3-8.4	2244	0	~ 0.001	2570	2214	71	70	11	-
Ordovician (Oil reservoir)	Limestone	35	8.4-8.6	2342	18	6	2970	1504	95	32	5.3	-
Ordovician (Cap rock)	Claystone, marl, limestone	35-37	8.6-9.3	2540	3	~ 0.001	2628	2264	74	74	13	-
Deimena (Reservoir-1)	Sandstone	37	9.3-9.7	2340	21	150	2874	1302	68	23	4	6.6
Deimena (Reservoir-2)	Sandstone	37	9.7-9.8	2400	17	60	2813	1162	85	25	3.2	5.4
Deimena (Reservoir-3)	Sandstone	37-38	9.8-10	2340	24	240	2812	1280	106	35	3.8	6.4
Cambrian	Siltstone	38-41	10-11.2	2324	0-19	0.2-23	2746	1450	81	30	4.9	-
Basement	Granite	41-…	11.2-…	2675	-	-	5800	3454	362	171	31.9	-

All formations except the Oil Reservoir are saturated with brine. Temperature **(T)** and pressure **(P)** of the formations top and bottom are shown (extrapolated by measured data and gradients reported for the reservoir and cap rock layers). ρ_{wet} is the bulk density of brine saturated rock samples. **ϕ** - average porosity; **κ** - average permeability; V_P and V_S - compressional (P) and shear (S) waves velocities respectively; Q_P and Q_S - quality factors of P- and S-waves (*White's theory from Udias, 1999; Waters, 1978; Haase and Stewart, 2004*) respectively; **μ** and **K** - shear and bulk moduli of dry rocks respectively (**K** estimated for reservoir formations)

Reservoir properties estimation

Dry P-wave velocities (V_{Pdry}), dry bulk density (ρ_{dry}), density of rock solid part (ρ_s) and porosity (**ϕ**) were estimated using measured properties at IFPEN petrophysical laboratory (**Shogenov et al., 2013a**) and reported data. Dry S-wave velocities (V_{Sdry}) and in situ rock physical parameters of CO_2 storage reservoir rocks, as wet P- and S-wave velocities (V_{Pwet} and V_{Swet}, respectively), wet bulk density (ρ_{wet}), wet bulk modulus (K_{wet}) and shear modulus (**μ**) were estimated by rock physics theories:

$$K_{dry} = V_{Pdry}^2 \times \rho_{dry} - \frac{4}{3}\mu_{dry} \quad \text{, III}$$

$$K_{wet} = K_{dry} + \frac{\left(1 - \frac{K_{dry}}{K_0}\right)^2}{\frac{\phi}{K_{fl}} + \frac{1-\phi}{K_0} - \frac{K_{dry}}{K_0^2}} \quad \text{, II}$$

$$\rho_{dry} = m/V_{total} \quad \text{, IV}$$

$$K_{fl} = c^2 \times \rho_{fl} \quad \text{, V}$$

$$V_{P(wet/dry)} = \sqrt{\frac{K_{(wet/dry)} + \frac{4}{3}\mu_{(wet=dry)}}{\rho_{(wet/dry)}}} \quad \text{, I}$$

$$\mu_{dry} = V_{Sdry}^2 \times \rho_{dry} \quad \text{, VI}$$

$$V_{Sdry} = \frac{V_{Pdry}}{1.73} \quad \text{, VII}$$

$$\rho_{wet} = \rho_s \times (1-\phi) + \rho_{fl} \times \phi \quad \text{, VIII}$$

$$\rho_s = m/(V_{total} - V_{pores}) \quad \text{, IX}$$

ρ_{fl} = ρ_w+S(0.668+0.44S+10-6(300P-2400PS+T(80+3T-3300S-13P+47PS))) , **X**

ρ_w=1+10-6(-80T-3.3T2+0.00175T3+489P-2TP+0.016T2P-1.3 • 10-5T3P-0.333P2-0.002TP2) , **XI**

$$V_{Swet} = \sqrt{\frac{\mu_{dry}}{\rho_{wet}}} \quad \text{, XII}$$

K_{fl}-bulk modulus of brine at in situ conditions, **c** -speed of sound in the fluid at in situ conditions within the E6 reservoir (1633 m/s), K_0-bulk modulus of rock sample grains. Average K_0 of quartz = 37 GPa, **m**-sample weight (g), V_{total}-sample total volume (cm³), V_{pores}-sample pore volume (cm³), ρ_{fl}-density of brine at in situ conditions (within the reservoir layers 1066.7 kg/m³), **S**-weight fraction (ppm/1000000) of sodium chloride(99000 ppm)

Non-reservoir properties estimation

To evaluate specific properties of non-reservoir layers we have used reported active seismic data (V_{Pwet}) and reported laboratory measurements of dry and wet samples (Oil reservoir), obtained from the well E6-1/84, and reported measurements of more than 2000 samples of Baltic Basin (**Shogenova et al., 2001**).

Devonian sandstones

$$V_{Swet} = 0.804 \times V_P - 0.856 \ \text{(km/s)} \quad \text{, XIII}$$

Silurian shales

$$\rho_{wet(shales)} = -0.0261 \times V_{Pwet}^2 + 0.373 \times V_{Pwet} + 1.458 \quad \text{, XIV}$$

$$V_{Swet} = 0.862 \times V_P - 1.172 \ \text{(km/s)} \quad \text{, XV}$$

Ordovician oil limestones

$$V_{Swet} = -0.055 \times V_{Pwet}^2 + 1.017 \times V_{Pwet} - 1.031 \ \text{(km/s)} \quad \text{, XVI}$$

Ordovician claystones, marlstones and limestones , **VIII, XV**

Cambrian siltstones , **VIII, XII**

Basement

$$\rho_{wet} = 1.6612 \times V_{Pwet} - 0.4721 \times V_{Pwet}^2 + 0.0671 \times V_{Pwet}^3 - 0.0043 \times V_{Pwet}^4 + 0.000106 \times V_{Pwet}^5 \quad \text{, XVII} \ \text{(kg/m}^3\text{)}$$

$$V_{Swet} = 0.7858 - 1.2344 \times V_{Pwet} + 0.7949 \times V_{Pwet}^2 - 0.1238 \times V_{Pwet}^3 + 0.0064 \times V_{Pwet}^4 \quad \text{, XVIII} \ \text{(km/s)}$$

2.2 PROPERTIES AFTER CO_2 SATURATION

V_P
Quality factors
Attenuation
Estimated by → White's mesoscopic rock physics theory (**White, 1975**). This theory provides realistic V_P and Q as a function of porosity, dry rock properties, gas saturation, fluid viscosity, permeability and dominant frequency of the seismic pulse **(Carcione et al., 2003, 2006, 2007, 2012)**

V_S → **Equation XII**

Tabel 2. Seismic properties of the Deimena Sandstone Formation of Middle Cambrian partially saturated with CO_2

Formation		Fluid saturation	ρ (kg/m³)	V_P (m/s)	V_S (m/s)	Q_P	Q_S
Middle Cambrian Deimena Sandstone Formation	RESERVOIR-1	Brine (99%)+CO2 (1%)	2341	2642	1328	68	23
		Brine (95%)+CO2 (5%)	2335	2410	1330	45	18
		Brine (85%)+CO2 (15%)	2325	2325	1320	89	38
		Brine (50%)+CO2 (50%)	2290	2295	1318	866	380
		Brine (10%)+CO2 (90%)	2250	2310	1328	97472	43007
	RESERVOIR-2	Brine (99%)+CO2 (1%)	2400	2554	1185	85	25
		Brine (95%)+CO2 (5%)	2397	2240	1194	41	16
		Brine (85%)+CO2 (15%)	2390	2114	1180	72	30
		Brine (50%)+CO2 (50%)	2362	2055	1170	642	279
		Brine (10%)+CO2 (90%)	2330	2057	1180	68600	30070
	RESERVOIR-3	Brine (99%)+CO2 (1%)	2338	2615	1297	106	35
		Brine (95%)+CO2 (5%)	2334	2383	1304	57	23
		Brine (85%)+CO2 (15%)	2324	2290	1295	105	45
		Brine (50%)+CO2 (50%)	2287	2260	1295	976	428
		Brine (10%)+CO2 (90%)	2245	2270	1305	107246	47297

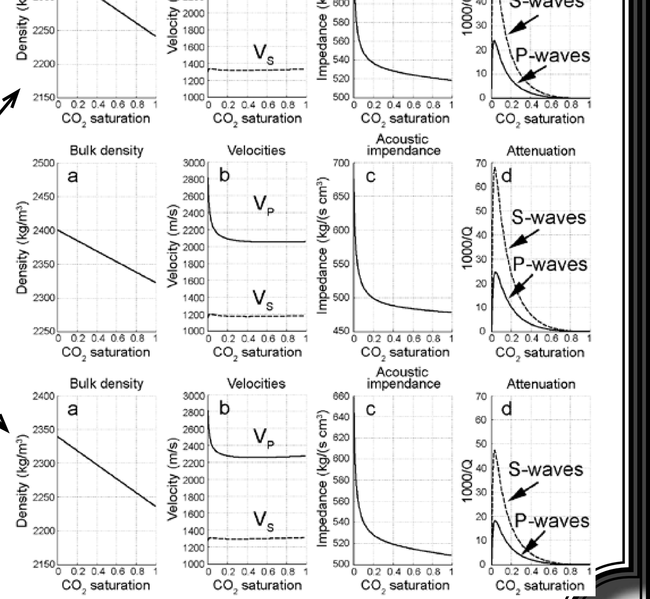

Fig. 5. Estimated bulk density **(a)**, P- and S-wave velocities (V_P and V_S respecttively) **(b)**, acoustic impedance **(c)** and attenuation **(d)** of the Deimena sandstones vs CO_2 saturation for different reservoir sub-layers. Brine and CO_2 are the saturating fluids

2.3 SYNTHETIC SEISMIC SECTION

The 2D viscoelastic wave equation were solved with a 4th-order Runge-Kutta time-stepping scheme and the staggered Fourier method for computing the spatial derivatives, which is noise-free in the dynamic range where regular grids generate artifacts that may have amplitudes similar to those of physical arrivals (**Carcione, 2007**).
Plane-wave simulations approximating non-migrated zero-offset sections by triggering simultaneously sources located in each grid point of the upper edge of the numerical mesh represented by the model were applied. This procedure produces a plane wave propagating downward. Every time the plane-wave impinges upon the interface between two different formations, it is reflected back to upper edge of the geological model, coinciding with the sea surface, where seismic sensors record the seismic wave-field.
Difference and NRMS sections of 4D seismic data are effective tools to indicate differences such as phase shifts of amplitude variations in time-lapse datasets (**Picotti et al., 2012**). NRMS difference technique was used to compare seismic datasets before and after CO_2 injection simulating seismic acquisitions at different times over the same studied area (**Kragh and Christie, 2002**). A Ricker wavelet with a dominant frequency of 35 Hz was applied as source time history.

III. RESULTS

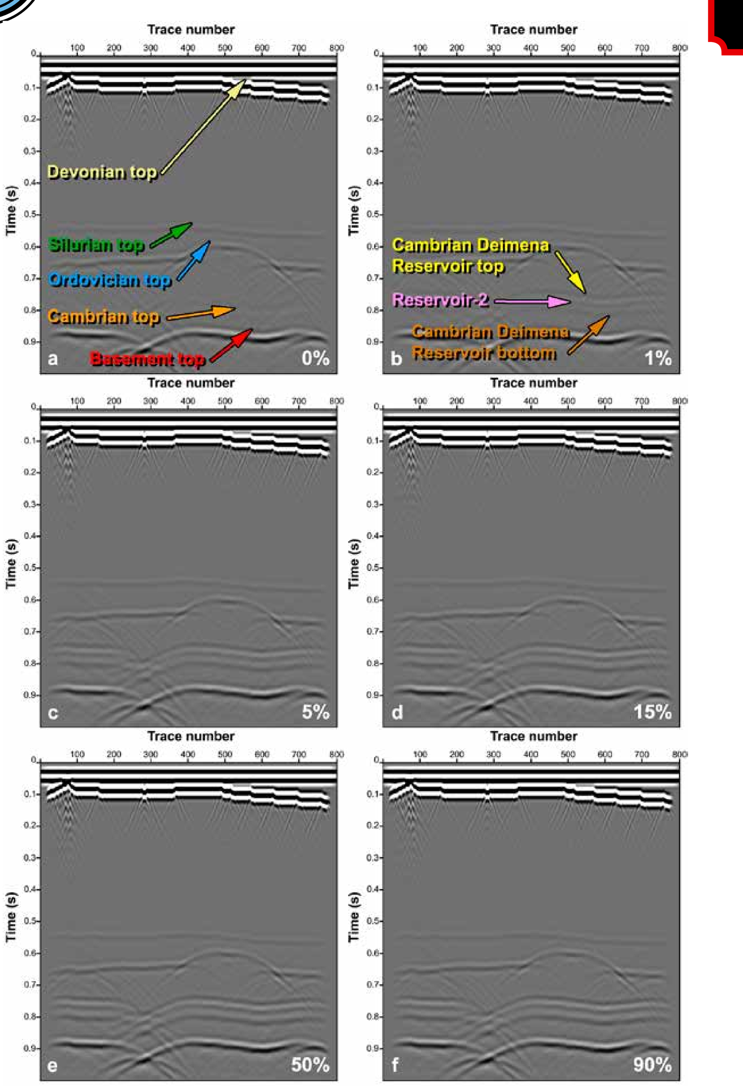

Fig. 6. Synthetic plane-wave sections with 0% **(a)**, 1% **(b)**, 5% **(c)**, 15% **(d)**, 50% **(e)**, 90% **(f)** of CO_2 saturation. Approximate locations of the top of all geological formations except for reservoir **(a)** and the top and bottom of the Cambrian Deimena Sandstone Reservoir, and middle part of reservoir formation Reservoir-2, saturated with CO_2 **(b)** are indicated

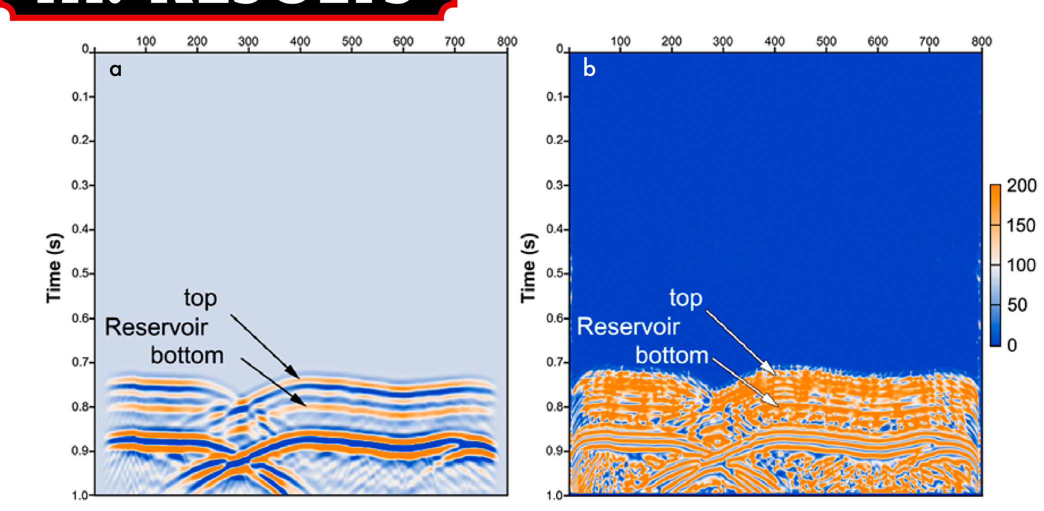

Fig. 7. Difference between the synthetic baseline (0% of CO_2) and the synthetic seismic line with 5% of CO_2 in the saturating fluid **(a)** and corresponding NRMS section **(b)**. Seismic data are computed with the geological model of **Figure 4** and seismic properties given in **Table 1** and **Table 2**. The arrows indicate the reservoir top and bottom. The signal caused by the presence of CO_2

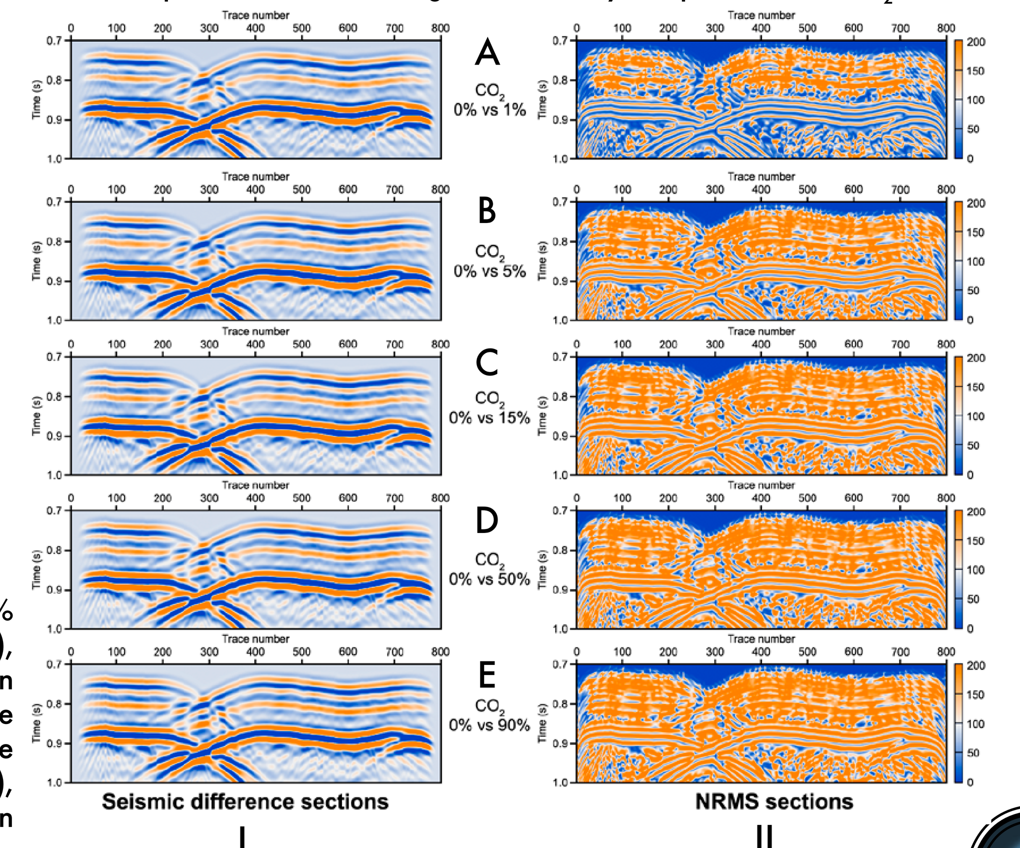

Fig. 8. Difference between the synthetic baseline (0% of CO_2) and the synthetic seismic lines with 1% **(I-A)**, 5% **(I-B)**, 15% **(I-C)**, 50% **(I-D)** and 90% **(I-E)** of CO_2 in the porous space presented on the left part of the figure **(I)**. The corresponding NRMS sections are shown on the right part of the figure **(II)** in panels **(II-A)**, **(II-B)**, **(II-C)**, **(II-D)** and **(II-E)**, respectively. Panels are focusing on reservoir level of the section

IV. DISCUSSION

Behaviour of the seismic response and its ability to visualise a small quantities of injected CO_2 were explored using the plane-wave, difference and NRMS seismic sections in the modelled E6 structure reservoir. Arrival times and reflection strength from the reservoir and deeper formations vary with continuous changes of seismic properties due to the increasing CO_2 saturation.
This phenomenon is due to changing of magnitude of the reflection coefficient with increasing of CO_2 content, already with 1% of CO_2 saturation. Thin interbeds within the Reservoir (1, 2 and 3) implemented in the model and the Oil Reservoir (**Figure 4**) were impossible to define on the seismic sections due to the relatively low frequency of the seismic source (35 Hz), resulting in a single reflection. However, Reservoir-2 was reflected (as one reflection) and detectible on the plane-wave sections after injection of CO_2 **(Fig. 6)**. Reflectors on the difference section **(Fig. 7)** characterized by two-way travel times lower than the reservoir are not influenced by the presence of CO_2 and give zero signal. The presence of CO_2 in the reservoir causes decrease of the P-wave velocity compared to the brine saturated Deimena sandstone and a variation of the quality factors **(Table 2)**. These differences in the seismic properties determine a non-zero amplitude in the difference section for the reservoir and the reflectors located at higher depth. The lower part of the difference and NRMS sections were affected by multiple reflections **(Fig. 7, 8)**. Difference between 1% and 15% of CO_2 saturation is cleraly detectible, while after 15% it is difficult to monitor CO_2 saturation change. This phenomena could be explained by relatively stable V_P and attenuation values in reservoir rocks after fluid saturation of 15% of CO_2 **(Fig. 5 b, d)**.

V. CONCLUSION

The synthetic plane-wave and difference sections clearly indicate the presence of CO_2 in the reservoir Formation in the E6 offshore structure for various saturation levels. Nevertheless, NRMS, which is one of the best methods suited for time-lapse seismic analysis, is affected by the presence of numerical noise and multiples. Our study shows effectiveness of seismic method to monitor the presence of CO_2 in the E6 Baltic Sea offshore structure already from the first stages of the injection (1% of reservoir fluid saturation). This study is important for developing an optimal seismic monitoring plan in the studied area.

REFERENCES

1) **Carcione**, J. M., Helle, H. B., and Pham, N. H., [**2003**]. White's model for wave propagation in partially saturated rocks: Comparison with poroelastic numerical experiments. Geophysics 68, 1389-1398.
2) **Carcione**, J. M., S. Picotti, D., Gei and G., Rossi, [**2006**], Physics and Seismic Modeling for Monitoring CO_2 Storage, Pure appl. geophys., 163, 175–207.
3) **Carcione**, J. M., [**2007**] Wave fields in real media: wave propagation in anisotropic, anelastic, porous and electromagnetic media. 2nd edition, revised and extended, Handbook of Geophysical Exploration, vol. 38, Elsevier, Amsterdam, 1-514.
4) **Carcione**, J. M., D., Gei, S., Picotti, and A. Michelini, [**2012**], Cross-hole electromagnetic and seismic modeling for CO_2 detection and monitoring in a saline aquifer, Journal of Petroleum Science and Engineering, accepted for publication, Volume 100, 162-172.
5) **Haase**, A., and R., Stewart., **2004**, Attenuation estimates from vsp and log data, 74th ann. Internat. Mtg., SEG Exp. Abstr, 2497–2500.
6) **Kragh**, E. and P. Christie, [**2002**] Seismic repeatability, normalized RMS and predictability. The Leading Edge, 21, 642-647.
7) **Rossi**, G., Gei, D., Picotti, S. and Carcione, J.M. [**2008**] CO_2 storage at the Aztbach-Schwanenstadt gas field: a seismic monitoring feasibility study. First Break, 26, 45-51.
8) **Shogenov**, K., Shogenova, A., Vizika-Kavvadias, O. [**2013a**] Petrophysical properties and capacity of prospective structures for geological storage of CO_2 onshore and offshore Baltic. Elsevier, Energy Procedia, in press, 1-8.
9) **Shogenov**, K., Shogenova, A., Vizika-Kavvadias, O. [**2013b**]. Potential structures for CO_2 geological storage in the Baltic Sea: case study offshore Latvia. Bulletin of The Geological Society of Finland, accepted.
10) **Shogenova**, A., Šliaupa, S., Rasteniene, V., Jõeleht, A., Kirsimäe, K., Bitjukova, L., Lashkova, L., Zabele, A., Freimanis, Hoth, P., Huenges, E. [**2001**] . Elastic properties of siliciclastic rocks from Baltic Cambrian basin. In: Extended Abstracts, Volume 1, EAGE 63rd Conference and Technical Exhibition. European Association of Geoscientists & Engineers, Amsterdam, The Netherlands. N-24, 1–4.
11) **Udias**, A., [**1999**] , Principles of seismology: Cambridge University Press.
12) **Waters**, K., [**1978**] , Reflection Seismology: A tool for energy resource exploration, John Wiley and Sons, New York, NY.
13) **White**, J. E. [**1975**] Computed seismic speeds and attenuation in rocks with partial gas saturation. Geophysics, 40, 224–232.

ACKNOWLEDGEMENTS

This study was funded by EU FP7 Marie Curie Research Training Network "Quantitative Estimation of Earth's Seismic Sources and Structure" (QUEST), Contract No. 238007 and is a part of K. Shogenov PhD research. We are grateful to IFPEN (France) for petrophysical measurements and Dr. Alla Shogenova from Tallinn University of Technology for her kind revision.